Colloid Polym Sci (2015) 293:3611–3622
DOI 10.1007/s00396-015-3744-z

ORIGINAL CONTRIBUTION

Synthesis and characterization of a pH-responsive poly(ethylene glycol)-based hydrogel: acid degradation, equilibrium swelling, and absorption kinetic characteristics

Ernandes T. Tenório-Neto[1] · Marcos R. Guilherme[1] · Michele K. Lima-Tenório[1] · Débora B. Scariot[2] · Celso V. Nakamura[2] · Adley F. Rubira[1] · Marcos H. Kunita[1]

Received: 28 April 2015 / Revised: 9 August 2015 / Accepted: 11 August 2015 / Published online: 23 August 2015

Abstract We developed a pH-responsive, hydrogel based on poly(ethylene glycol) (PEG) covalently cross-linked with acrylic acid and *N′,N′*-dimethylacrylamide along with acid-labile groups. In the hydrogel, PEG plays a role as the key constituent. If its chains break, the polymer networks are destroyed. The pharmacological potential of these hydrogels were demonstrated by determining their water transport profile, modulus of elasticity, and cytotoxicity assay. The hydrogels showed a pseudo-Fickian behavior, a transport mechanism that occurs when the diffusion coefficient changes with the time and the swelling equilibrium is never fully reached. At pH 2, the PEG-richer hydrogels degraded and the scanning electron microscopy (SEM) images illustrated less-defined shapes than at pH 7 and 10. This morphological characteristic results of the hydrogel deconstruction owing to cleavage of ether bonds of the PEG chains unmaking its 3D polymer network. The proposed hydrogels were shown to be compatible to cells, indicating acceptable biocompatibility and an appropriate level of security for use in the biological environments. Furthermore, they showed structural changes in their polymer network in response to pH, which is an important characteristic for stimuli-triggered release of guest molecules.

Keywords Smart polymers · Hydrogel · PEG · pH responsiveness · Polymer gels · Water transport

✉ Marcos H. Kunita
mkunita@gmail.com

[1] Department of Chemistry, State University of Maringá, Av. Colombo, 5790, 87020-900 Maringá, Paraná, Brazil

[2] Department of Basic Sciences of Health, State University of Maringá, Av. Colombo, 5790, 87020-900 Maringá, Paraná, Brazil

Introduction

Hydrogels (called water-based gels or aqueous gels) are water absorbers of high performance because of their ability to absorb and retain a large volume of the liquid while maintaining a distinct 3D polymer network [1]. The capability of water absorption (swollen weight per dry weight) depends on the porosity, cross-linking density, and chemical nature of the polymer chains carrying functional groups such as $–NH_2$, –COOH, $–CONH_2$, and $–SO_3H$ [2]. Hydrogels may be prepared so that their physical–chemical characteristics (e.g., equilibrium swelling and absorption kinetic) respond to changes in their external environment, such as temperature [3], pH [4, 5], ionic strength [6], and so on. These materials show a wide variety of applications such as drug delivery [7], membranes for (bio)separation process [8], substrate for cell culture [9], and mucosal vaccines [10].

Polymer systems based on poly(ethylene glycol) (PEG) are among the most widely studied in the biomedical applications, owing to their biocompatibility and low toxicity [11]. PEG is a neutral, nontoxic, water-soluble polymer approved by the US Food and Drug Administration (FDA) for a variety of clinical uses, such as carrier and excipient in the pharmaceutical, cosmetic, and food products [5, 11]. PEG has also been used in drug delivery, tissue engineering scaffolds, surface functionalization, and so forth [12, 13]. Researchers in the area of biotechnology have focused on thermo-sensitive, pH-responsive, and (bio)degradable hydrogels that may be obtained from PEG [14]. An efficient strategy using polymers as starting monomers for creating hydrogel network is based on the chemical modification of functional groups. PEG has two hydroxyl end-groups, which can be converted to other polymerizable, reactive groups, such as methyloxyl, carboxyl, amine, thiol, azide, vinyl sulfone, azide, acetylene, and acrylate [15–17].

This work aimed at creating a covalent hydrogel based on PEG, acrylic acid (AAc), and *N′,N′*-dimethylacrylamide (DMAAm) that shows pH-responsive structural changes, which is a valuable characteristic for stimuli-triggered release of guest molecules from the polymers into aqueous environments. In the water-swellable polymers, the release of solutes is driven by the mechanisms of diffusion, macromolecular relaxation, and erosion [18, 19]. These mechanisms depend on physical–chemical interactions between the hydrogel and the surrounding liquid. In addition, the erosion is the result of either mass loss or burst of vesicular structure due to osmotic pressure during the swelling [20]. For some authors, the erosion mechanism is similar to that of degradation. The control of the mechanism by which the hydrogel undergoes degradation may help in attaining sustained release characteristics [21, 22].

In order to prepare a degradable hydrogel, PEG was chosen as a key constituent acting as a pillar on polymer network. If its chains break, the polymer network crumbles. AAc is the ionic monomer, and DMAAm was used owing to its good gel-forming capacity. Before gelation, PEG was vinyl-modified with glycidyl methacrylate (GMA) (^{GMA}PEG) and subsequently cross-linked/polymerized with sodium acrylate (SA) and DMAAm. On the scientific basis, it has not yet found reports on hydrogel with such architecture.

Experimental

Materials

PEG Mn 950–1050 g mol^{-1}, GMA, sodium persulfate ($Na_2S_2O_8$), DMAAm, and AAc were purchased from Sigma-Aldrich. Acetone and sodium hydroxide (NaOH) in pellets were supplied by Fmaia. All chemicals were of analytical grades and used without further purification.

Evaluation of chemical route for modifying PEG with GMA

PEG (9.75 g) was added to 35 mL of water at room temperature while stirring. The temperature of the mixture was increased up to 50 °C, and the pH was adjusted to 10.5 with addition of 1.0 mol L^{-1} NaOH solution. Then, 2.7 mL of GMA was introduced into the mixture. It was observed that the pH of the solution spontaneously decreased to approx. 7.0 after addition of GMA. In order to have more precise control over the reaction, two different investigations on the PEG modification were performed: (i) at pH 7.0, which was the pH the solution after addition of GMA, and (ii) where pH of the solution was readjusted up to pH 10.5 by adding NaOH. The solution of PEG with GMA was left to react for 6 h under stirring of 300 rpm. Later, the solution was labeled ^{GMA}PEG solution. The product was separated by centrifugation and freeze-dried for 24 h for chemical characterization by spectroscopy.

Preparation of SA from AAc

In the hydrogel-forming solutions, acrylate salt was used instead of acrylic acid in order to prevent overheating, by acid addition, over gelation at 70 °C. In a common example of neutralization, 50 mL of AAc were solubilized in acetone at room temperature under continuous stirring of 300 rpm. Then, 28.6 g (0.71 mol) of NaOH were slowly added to the stirred solution. After few a minutes, the clear solution turned to a whitish suspension, as a result of the salt precipitation. The precipitate was filtered under vacuum and left to dry in a ventilated oven at 35 °C for 48 h.

Synthesis of hydrogels based on ^{GMA}PEG

The experimental conditions of hydrogel synthesis were chosen on the basis of spectroscopic data for modification of PEG with GMA (^{GMA}PEG). Result from those studies motived us to use the ^{GMA}PEG synthesized at pH 7.0, as a cross-linker agent, because ^{GMA}PEG structure showed only two isomers (as shall be seen in "Results and discussions"). Moreover, recently prepared ^{GMA}PEG solutions were employed to prepare the hydrogel. In view of this, a two-step synthesis was performed. In the first step, 16 g of PEG (16 mmol) were added to 80 mL of water at 50 °C while stirring. The pH of the mixture was adjusted to pH 10.5 with NaOH solution at 1.0 mol L^{-1} concentration. After the solubilization, 4.8 mL of GMA (32.4 mmol) were introduced, causing a spontaneous decrease in pH to ca. 7. The solution of PEG with GMA was left to react for 6 h under mild stirring. In the second step, the ^{GMA}PEG solutions were used to produce the hydrogels using volumes of 5 and 10 mL, as shown in Table 1. The final volume of solvent used in the hydrogel-forming solutions was 10 mL. In the case of hydrogels prepared with 5 mL of solution, the volume was made up to 10 mL with water. Then, DMAAm, SA (Table 1), and $Na_2S_2O_8$ (0.03 g) were added to ^{GMA}PEG solution at 70 °C and left to react for 30 min, forming a transparent material. The thus obtained hydrogels was washed with distilled water and stored at 15 °C before swelling experiments.

Stress–strain measurements

The mechanical tests were performed on the hydrogels free from air bubbles or physical imperfections. This was verified visually. Mechanical tests were considered as being the measured force for compressing the hydrogels to 1 mm deformation using a texture analyzer TAX.T2i equipped with a 5 kg load cell. The apparatus was equipped with a circular probe of

Table 1 Volumes of ^{GMA}PEG solution and amounts of DMAAm and SA used for gelation

Sample name	^{GMA}PEG solution (mL)	DMAAm (g)	SA (g)
P1D1A1	5.0	0.5	0.6
P1D1A2	5.0	0.5	1.2
P1D2A1	5.0	1.0	0.5
P1D2A2	5.0	1.0	1.2
P2D1A1	10.0	0.5	0.6
P2D1A2	10.0	0.5	1.2
P2D2A1	10.0	1.0	0.6
P2D2A2	10.0	1.0	1.2
P2D2	10.0	1.0	xx
P2A2[a]	10.0	xx	1.2

[a] Hydrogel not formed

0.5 mm diameter (P/0.5), which was programmed to descend onto gel surface moving at a constant speed of 2 mm s^{-1}. The hydrogels were cut into small pieces with 10-mm height, 100-mm^2 surface dimensions. Their compressive strength was performed at 25 °C. The stress–strain measurements were done in triplicate, shortly after polymerization. Each measurement was performed in less than 1 min to prevent water loss by the hydrogel over the experiment. The force necessary for compressing the hydrogels at 1 mm was recorded, and the stress values(s) were determined using the Eq. (1):

$$\sigma = \frac{F}{A} = E\varepsilon \quad (1)$$

where F is the force and A is the cross-sectional area of the hydrogel; E is the elastic modulus, and ε is relative deformation of the sample ($\Delta l/l_0$).

Swelling kinetics of ^{GMA}PEG hydrogels (water absorption capacity)

The swelling degree (SW) of the hydrogels were investigated by immersing the 1-cm^3 dry samples of known mass into buffer solutions of pH 2, 7, and 10, in dependence on time at 36.5 °C. The hydrogels were withdrawn from the solution buffers; the excess water droplets on the surface were wiped off carefully, and the samples were weighed at each new time step. This procedure was done until to achieve the swelling equilibrium. SW of ^{GMA}PEG hydrogels with different compositions was obtained from the Eq. (2), correlating the water mass within the hydrogel at any time (M_t) to the initial mass of hydrogel (M_0).

$$SW = \frac{M_t - M_o}{M_o} \quad (2)$$

Characterizations

FTIR

The Fourier transform infrared spectroscopy (FTIR) spectra were recorded in a Bruker spectrometer model Vertex 70V. Powdered samples were prepared into pellets with KBr. The scan range varied from 400 to 4000 cm^{-1}, and 128 scans were run for each spectrum to reach the resolution of 4 cm^{-1}.

^{1}H-NMR and solid-state ^{13}C-CP/MAS

The ^{1}H-NMR spectra were recorded in a Varian spectrometer, model Mercury Plus BB 300 MHz, using a frequency of 300.059 MHz for ^{1}H nucleus, an angle pulse of 90°, and a relaxation delay of 30 s. The spectra were obtained with $CDCl_3$ solutions containing 20 mg L^{-1} of sample. The chemical shift was reported as δ values (ppm). The solid-state ^{13}C cross-polarization magic angle spinning (^{13}C-CP/MAS) NMR spectra of the powdered hydrogels were obtained using an angle pulse of 37°, a frequency of 75.45 MHz for ^{13}C nucleus, a contact time of 3 ms, and a relaxation time of 3 s.

SEM

The hydrogels were swollen to equilibrium in water prior to scanning electron microscopy (SEM) imaging. They were withdrawn from water and immediately frozen by immersion in liquid nitrogen before being lyophilized for 72 h. Under these conditions, it is supposed that the morphology of the swollen hydrogels is maintained. The samples were sputter-coated with a thin layer of gold, and the SEM images were obtained in a scanning electron microscope (Shimadzu, model SS550 Superscan) by applying an acceleration voltage of 15 kV and a current intensity of 30 μA.

Cytotoxicity measurement

Cytotoxic effects were evaluated against VERO line cells, originated from kidney of African green monkey. The cells were cultivated in Dulbecco's modified Eagle's medium (DMEM) with 10 % fetal calf serum (FCS) at 37 °C and 5 % CO_2. Approximately 2.5×10^5 cells were obtained by trypsinization and added to a 96-well plate for 24 h, using the same conditions described previously. Later, the compounds in different concentrations were added and incubated for 72 h. After that, MTT (Amresco®) solution at 2 mg mL^{-1} concentration was maintained in the wells for 4 h for reading of the absorbance at 570 nm, in a microplate spectrophotometer (BioTek PowerWave XS).

Results and discussions

Characterization of PEG modified with GMA

Figure 1 shows the FTIR spectra of GMA, ^{GMA}PEG, and PEG in the spectral range of 2000 to 800 cm^{-1}. The spectra of ^{GMA}PEG synthesized at pH 7 and 10.5 showed the same characteristics. The bands at 1720 and 1640 cm^{-1} in the spectra of ^{GMA}PEG were attributed to stretching vibrations of carbonyl groups (νC=O) and vinyl groups (C=C), respectively [23, 24]. These signals correspond to conjugated esters derived from GMA moieties. Furthermore, in the same spectrum, the bands at 910 and 860 cm^{-1}, owing to ν_{as}C–C and νC–O of the epoxy ring, respectively, completely disappeared [16, 25]. These spectral changes indicated that PEG reacted with GMA by an epoxide ring-opening mechanism.

The chemical reaction of PEG with GMA was also analyzed by ^{1}H-NMR spectroscopy (Fig. 2). For a more detailed analysis, a scheme of the product resultant of the PEG reaction with GMA was shown in the inset.

The signals at δ 2.67, δ 2.84, and δ 3.23 in the spectrum of GMA were attributed to hydrogen from epoxide ring (6′, 6″, and 5′, respectively). These signals were not observed in the spectra of ^{GMA}PEG.

The signals at δ 6.17 and δ 5.74 in the spectra of ^{GMA}PEG modified at pH 7 were assigned to vinyl carbon-linked hydrogen from both (i) and (ii) isomers (inset). The signal at δ 1.94, in the same spectrum, corresponded to methyl carbon-linked hydrogen from vinyl carbons. These isomers result of the epoxide ring-opening mechanism [17]. Other signals of the ^{GMA}PEG structure were overlapped by hydrogen signals from PEG.

The signals that give information on the PEG reaction at pH 10 were observed at δ 5.67 and δ 5.36. They refer to hydrogen from vinyl groups of (iii) isomer (inset), which is a reaction product of the transesterification mechanism [26, 27]. A schema suggesting the chemical structure of the isomers resultant from PEG reaction with GMA as a function of pH was proposed in Fig. 3.

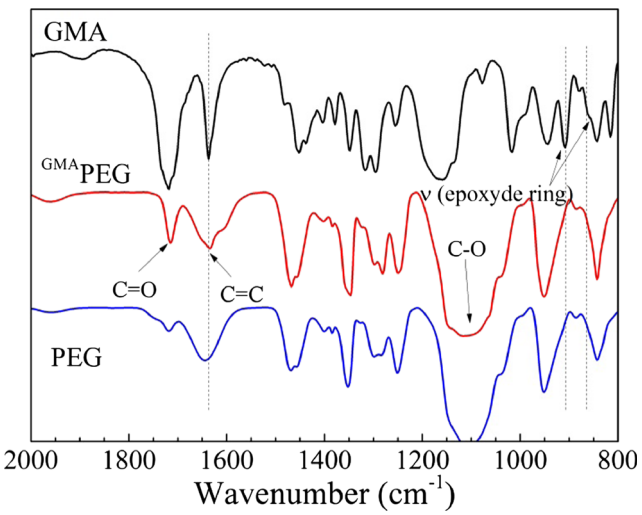

Fig. 1 FTIR spectra of GMA, ^{GMA}PEG, and PEG in the spectral range of 2000 to 800 cm^{-1}

At pH 10.5, three different isomers were obtained: (1) vinyl methacrylate of PEG, (2) 3-methacryloyl-1-glyceryl ether of PEG, and (3) 3-methacryloyl-2-glyceryl ether of PEG. The (1) and (2) isomers result from ring-opening reaction, and the (3) isomer originates from transesterification reaction. From a chemical point of view, the modification of PEG at pH 7 seems to be more interesting for further gelation, for two reasons. The first and most important reason is that the PEG reaction with GMA may be processed at a pH close to that of the pure water. The second reason is that the two isomers from epoxide ring-opening reaction (1, 2) carry hydroxyl groups in their chemical structures which could interact with water by way of hydrogen bonds within the swollen hydrogel. Thus, for hydrogel synthesis, the modification of PEG was performed at pH 7 in order to obtain preferably isomers from epoxide ring-opening reaction.

Characterization of hydrogels based on ^{GMA}PEG

Figure 4 shows the solid-state ^{13}C-CP/MAS spectra of the P2D2 and P2D2A2 hydrogels. The corresponding signal of carbonyl groups in the spectrum of P2D2 hydrogel was visualized at δ 178. This signal was attributed to C=O from both ^{GMA}PEG and DMAAm (f+h). The signal at δ 184 in the spectra of P2D2A2 was assigned to C=O from AAc (g) [28].

The signals between δ 60 and δ 80 were attributed to carbons linked to oxygen (CH-O and CH_2-O) and the signal at δ 19 (e) was ascribed to methyl group. Both of them were corresponded to ^{GMA}PEG structure [29]. In the same spectra, the signals at δ 45 and 37 ppm were assigned to carbons in the main chain of the hydrogel network (CH and CH_2, respectively) [30, 31]. Moreover, side band spinning effect (*) was associated with signals at δ 235 and δ 119, which are symmetric to the carbonyl group at δ 178 [32, 33]. From these spectroscopic data, a simplified schema suggesting the structure of the ^{GMA}PEG-based hydrogel was shown in Fig. 5.

Swelling performance

Figure 6 shows the swelling kinetics of the hydrogels in buffer solutions with pH 2, 7, and 10 at 36.5 °C. As a general trend, all hydrogels showed SW values higher at pH 10 and lower at pH 2. This effect may be associated with the ionization of the carboxylic groups (COOH) of AAc changing to acrylate ions (COO^-). In the alkaline medium, the COOH groups are ionized to form COO^- generating electrostatic repulsion forces among the polymer chains. As a result, the hydrogel affinity for water increases. However, at pH 2, there is an excess of H^+

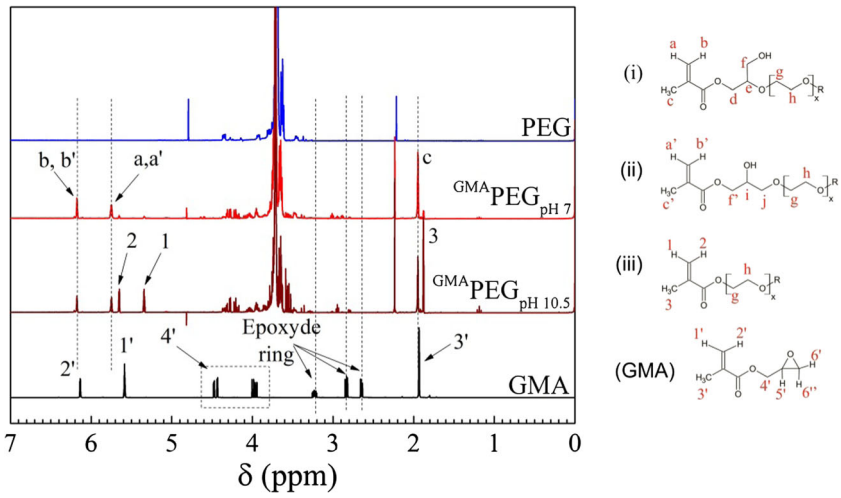

Fig. 2 ^{1}H-NMR spectra of PEG, ^{GMA}PEG modified at pH 7 and 10, and GMA. *Inset*: product resultant of the PEG reaction with GMA at pH 7 and 10.5

ions, and consequently, COO^{-} is converted to form COOH, leading to network hydrophilicity reduction [34, 35] This assumption is confirmed by comparing the hydrogels made of P2D2, P2D2A1, and P2D2A2 (Fig. 6i, g, h, respectively).

In Fig. 6i, the P2D2 hydrogel (without AAc) did not show significant SW changes by changing the pH of the surrounding liquid. However, the P2D2A1 and P2D2A2 hydrogels (both with AAc) showed higher swelling degree at pH 7 and 10. At pH 2, both of them showed lower SW, as a result of hydrogen bonds between the COOH groups [36, 37].

The effect of ^{GMA}PEG on the swelling performance also was investigated. The water absorption capacity of the hydrogels increases when the amount of ^{GMA}PEG decreases. This effect can be better visualized at pH 10. For example, the P1D1A1 hydrogel (Fig. 6a) showed SW value of ca. 8 The P2D1A1 hydrogel (Fig. 6e), which has higher amount of ^{GMA}PEG, showed SW value of ca. 6. The same effect also was found in both the P1D1A2 and the P2D1A2 hydrogels. The chemical nature of the polymer network forming the hydrogel affects SW but the cross-linking density also changes its water absorption performance [38]. ^{GMA}PEG has potential cross-linking points, owing to vinyl groups introduced by modification reaction. Larger amount of ^{GMA}PEG added for gelation results in a more densely cross-linked PEG network and thus in a lower SW.

In the acidic solutions, the hydrogel networks with larger amount of ^{GMA}PEG (Fig. 6e, f, g, h) started to crumble after achieving the swelling equilibrium. This fact may be associated to ester groups in ^{GMA}PEG. Under those conditions, the covalent bonds that form the main structure of the hydrogel can be destroyed by decreasing the swelling pH, as a result of acidic hydrolysis of ester groups. The breakage of ^{GMA}PEG, which is a key constituent of network, causes degradation of the cross-linked polymer network. Poon and co-workers have reported the hydrolysis in hydrogels containing poly(ethylene glycol) dimethacrylate [39]. Giammona and co-authors investigated both enzymatic and chemical hydrolysis on the PEG-derivative hydrogels [40]. In addition, Lee and co-workers reported the hydrogel degradation through ester bond hydrolysis resulting in the release of PEG and poly(acrylic acid-co-vinyl pyrrolidone) [41].

The hydrogel deconstruction seems to be similar to that reported by Lee and co-workers [41]. A schematic representation of the whole process of the hydrogel degradation is shown in Fig. 7.

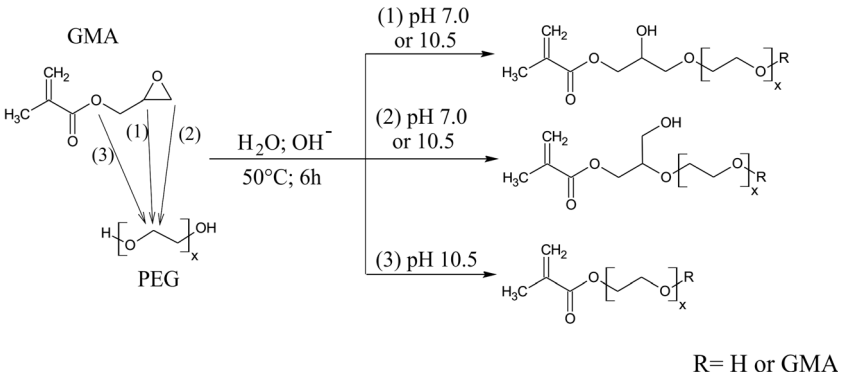

Fig. 3 Scheme of the chemical structure of isomers resultant from PEG reaction with GMA at pH 7 and 10.5

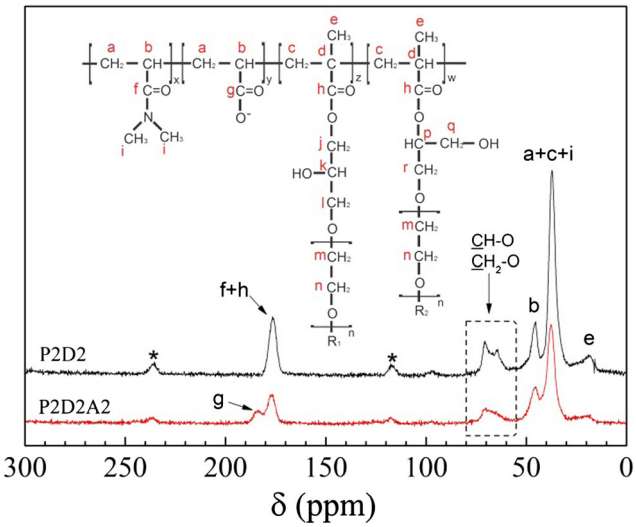

Fig. 4 Solid-state ^{13}C-CP/MAS NMR spectra of P2D2 and P2D2A2 hydrogels. Side band spinning effect (*asterisks*)

Studies of water transport

To have an insight into water transport through the hydrogels, the swelling mechanism was investigated. For water-swellable polymer networks, it can be described by power law model, applying the Eq. (3):

$$\frac{M_t}{M_{eq}} = kt^n \tag{3}$$

where n represents the diffusion coefficient that describes the specific transport mechanism, and k is a parameter related to diffusion coefficients. M_t and M_{eq} are the absorbed water masses by the hydrogel at a specific time and at equilibrium, respectively [42]. The plot of the relative mass of water diffused into hydrogel (M_t/M_{eq}) against time (t) gives both n and k values.

The Eq. (3) is a semiempirical, mathematical model that describes only the first 60 % of the absorbed water, when the water diffusion inwards the hydrogel linearly changes with time. Weibull function is an empirical equation that has been used as an alternative tool to describe overall profile of water absorption:

$$\frac{M_t}{M_{eq}} = 1 - e^{-[k_W(t-\tau_o)]d} \tag{4}$$

where τ_0 represents the time lag onset before swelling, d is related to mechanism, and k_W is associated to swelling rate constant [43, 44]. The Eq. (4) gives an insight into the diffusional mechanism and swelling rate [45, 46].

The fitting parameters were described in Table 2. The n and k parameters were obtained from Eq. (3) and the k_W parameter from Eq. (4). The n parameter has different conceptual meanings depending on geometrical shape of the material. For cylinder, which is the geometry of PEG-based hydrogels, when n=0.5, the swelling mechanism is termed as Fickian transport. This mechanism is characterized when the solvent diffusion rate is slower than relaxation rate. If n=*1* (case II transport), the diffusion is faster than relaxation.

An intermediate state between diffusion and relaxation occurs when $0.5 < n < 1$ [47–49]. However, all hydrogels showed n<0.5, which indicates a pseudo-Fickian behavior. This mechanism is observed when the diffusion coefficient changes with the time, consequently, and time required to achieve the swelling equilibrium is very slow [50, 51]. This can be explained by inhomogeneity of the hydrogels. The skin and bulk of the sample could differ in morphology and

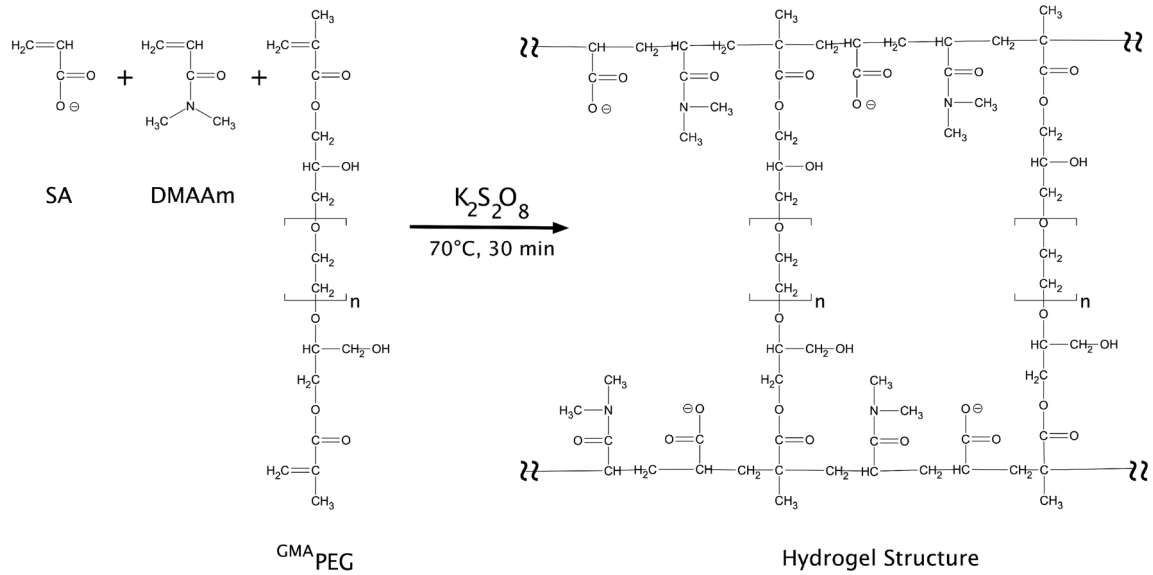

Fig. 5 Scheme of the chemical structure of ^{GMA}PEG-based hydrogel

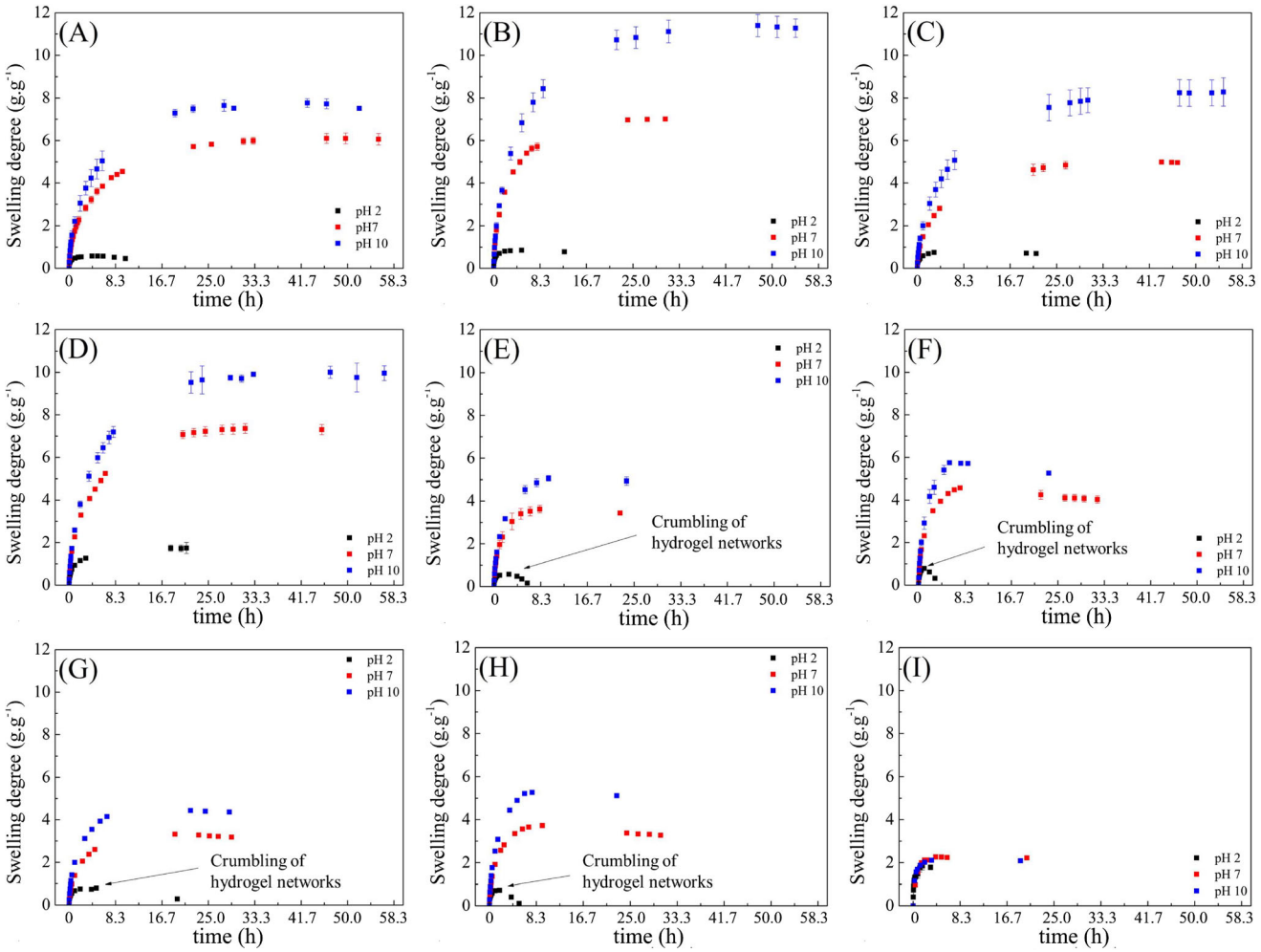

Fig. 6 Time-dependent swelling curves of hydrogels at the indicated pH at a temperature of 36.5 °C: **a** P1D1A1, **b** P1D1A2, **c** P1D2A1, **d** P1D2A2, **e** P2D1A1, **f** P2D1A2, **g** P2D2A1, **h** P2D2A2, and **i** P2D2

composition. Then, the diffusion process that occurs either on the surface or in the bulk of the hydrogel may be driven by a Fickian transport, but its combination may not be Fickian. Moreover, as the bulk increases, the influence of skin on the swelling decreases. This explains the time dependency of the coefficient diffusion [52, 53]. For hydrogels with AAc, both *n* and *d* values increase by increasing the pH, indicating a pH-dependent water transport mechanism.

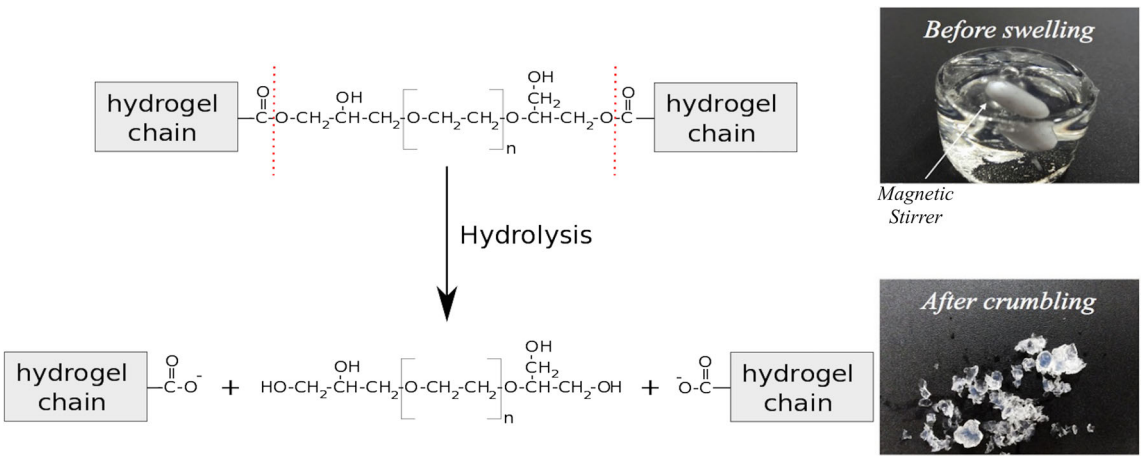

Fig. 7 Schematic representation of ^{GMA}PEG hydrogel degradation upon ester hydrolysis at pH 2. Digital photos of sample P2D2A1 taken after 500 min of swelling

Table 2 Fitting parameters of Eqs. (3) and (4) to swelling kinetics of hydrogels composed of ^{GMA}PEG, DMAAm, and SA at different pH at 36.5 °C

		Power law model		Weibull model	
Hydrogel	pH	n	k	d	k_W (min^{-1})
P1D1A1	2	0.100±0.002	0.723±0.003	0.295±0.018	0.572±0.095
	7	0.272±0.009	0.129±0.004	0.603±0.025	0.004±0.000[a]
	10	0.299±0.012	0.112±0.005	0.751±0.068	0.004±0.000[a]
P1D1A2	2	0.119±0.005	0.612±0.006	0.353±0.017	0.250±0.024
	7	0.308±0.013	0.124±0.005	0.581±0.018	0.006±0.000[a]
	10	0.358±0.017	0.074±0.004	0.683±0.021	0.003±0.000[a]
P1D2A1	2	0.083±0.007	0.661±0.009	0.311±0.046	0.289±0.097
	7	0.242±0.013	0.156±0.007	0.611±0.033	0.004±0.000[a]
	10	0.305±0.014	0.096±0.005	0.671±0.024	0.003±0.000[a]
P1D2A2	2	0.138±0.007	0.391±0.006	0.364±0.025	0.030±0.003
	7	0.296±0.015	0.116±0.005	0.680±0.043	0.004±0.000[a]
	10	0.347±0.017	0.080±0.005	0.704±0.025	0.003±0.000[a]
P2D1A1	2	0.094±0.002	0.691±0.003	0.376±0.022	0.508±0.070
	7	0.239±0.015	0.234±0.009	0.726±0.082	0.018±0.002
	10	0.284±0.015	0.167±0.007	0.714±0.058	0.012±0.001
P2D1A2	2	0.128±0.006	0.612±0.007	0.562±0.070	0.198±0.042
	7	0.270±0.014	0.204±0.007	0.674±0.041	0.014±0.001
	10	0.297±0.021	0.167±0.009	0.791±0.050	0.013±0.001
P2D2A1	2	0.106±0.004	0.608±0.005	0.341±0.023	0.281±0.040
	7	0.203±0.014	0.235±0.009	0.572±0.039	0.011±0.001
	10	0.259±0.013	0.185±0.007	0.629±0.032	0.011±0.001
P2D2A2	2	0.114±0.003	0.777±0.005	0.468±0.066	0.279±0.076
	7	0.231±0.014	0.244±0.008	0.650±0.038	0.014±0.001
	10	0.299±0.017	0.162±0.008	0.773±0.056	0.012±0.001
P2D2	2	0.271±0.006	0.433±0.005	0.458±0.044	0.220±0.029
	7	0.295±0.013	0.248±0.013	0.923±0.062	0.027±0.002
	10	0.162±0.019	0.460±0.035	0.602±0.034	0.072±0.005

[a] Standard deviation (SD) lower than 0.001

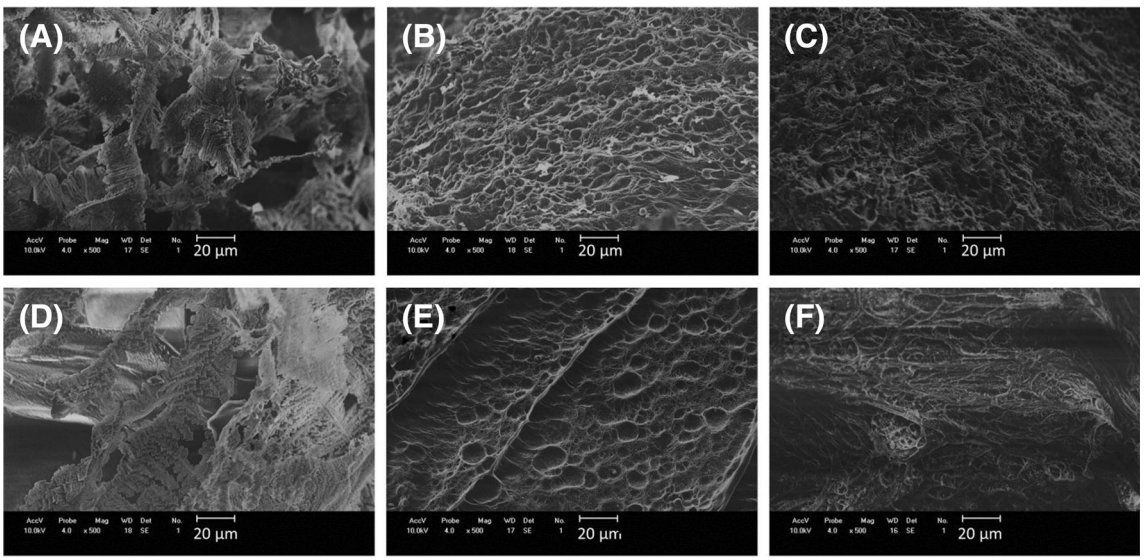

Fig. 8 SEM images of fractured frozen ^{GMA}PEG-based hydrogels after reaching the swelling equilibrium at pH 2, 7, and 10. **a** P1D1A1—pH 2, **b** P1D1A1—pH 7, **c** P1D1A1—pH 10, **d** P2D1A1—pH 2, **e** P2D1A1—pH 7, and **f** P2D1A1—pH 10

The parameter k from power law (Eq. (3)) and the swelling rate constant (k_W) from (Eq. (4)) are related, respectively, to the diffusion coefficient and velocity at which the hydrogel achieves the equilibrium. In Table 2, it is observed for all samples that k and k_W are higher at pH 2 than at any other pH studied. This means that the hydrogels achieve the equilibrium more quickly in the acidic medium. Furthermore, there was no significant difference on both k and k_W at pH 7 and pH 10. These observations suggest that the water absorption barely changes at pH≥7, in spite of the water transport mechanism showing more marked changes in both the acidic and the basic media.

Hydrogel morphology

Figure 8 shows the SEM micrographs of fractured frozen P1D1A1 and P2D1A1 hydrogels lyophilized after reaching the swelling equilibrium at different pH. For pH 7 and 10 (Fig. 8b, c, e, f), porous morphology was observed in any part of the fractured samples. This means that there are pores on and within the matrix. This attribute makes these hydrogels attractive as polymer carriers, because their porous structures allow the drug to diffuse into, through, and from the 3D polymer network. On the other hand, at pH 2 (Fig. 8a, d), the hydrogels degraded after swelling at pH 2, showing less-defined shapes. This morphological characteristic results in the cleavage of ester bonds of the ^{GMA}PEG chains deconstructing the hydrogel networks.

Mechanical behavior of the hydrogels

The correlation of stress and strain indicates an elastic deformation when the hydrogel undergoes a mechanical compression. In such a case, the strain is recovered by removing the applied stress. From a physical–chemical point of view, it is said that the strain is accommodated by the rearrangement of the polymer chains within the hydrogel. As a consequence, retractive elastic forces concomitantly develop in those polymer chains owing to their tendency to return to original configuration.

Table 3 Moduli of elasticity of hydrogels with different polymer compositions

Hydrogel	E (kPa)
P1D1A1	9.58±0.06
P1D1A2	14.46±0.06
P1D2A1	16.53±0.06
P1D2A2	31.88±0.11
P2D1A1	19.13±0.11
P2D1A2	15.20±0.06
P2D2A1	25.10±0.09
P2D2A2	40.08±0.16
P2D2	5.10±0.06

The modulus of elasticity (E) gives relevant information for development of hydrogels with excellent quality and stability to be applied in the biological environments. E was obtained from linear slope of the stress–strain curves (Fig. 9), and the data adjusted to Eq. (1) were summarized in Table 3.

The shape and characteristics of the stress–strain curves were affected by changing the amount of ^{GMA}PEG, AAc, or DMAAm in the hydrogel. The E values increased when larger amounts of those reactants were used. In such a case, the hydrogel becomes less soft; therefore, a loader is necessary to compress it to 1 mm.

The P1D1A1 hydrogel showed an E value of 9.58, but this value increased to 19.13 in the P2D1A hydrogel. With addition of more ^{GMA}PEG, the hydrogel becomes more cross-linked and thus less soft. This finding may be associated with SW values of those hydrogels. The P2D1A1 hydrogel is a less

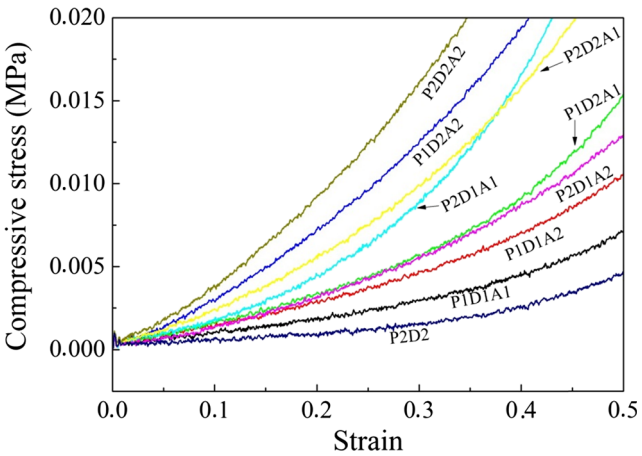

Fig. 9 Applied stress versus the strain curves of hydrogels with different compositions

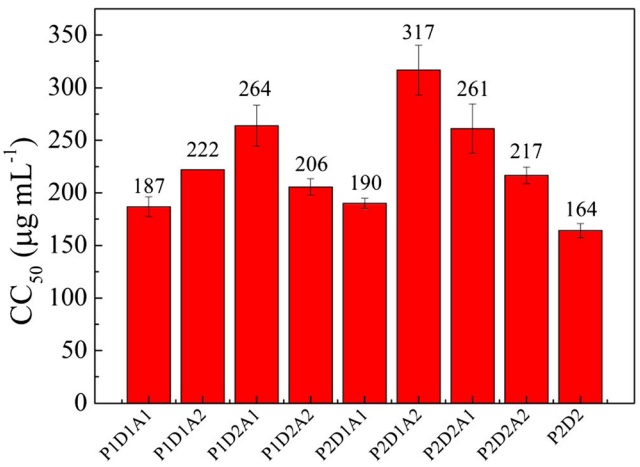

Fig. 10 Evaluation of cytotoxicity for ^{GMA}PEG hydrogels in VERO cells after 72 h of incubation at 37 °C and 5 % CO_2 by the MTT assay

efficient water absorber than the P1D1A1 hydrogel, because it has a less flexible, tighter polymer network that prevents its expansion in the liquid. The effect of acrylate groups on E (P1D2A1 and P2D2A1 hydrogels) is comparable to that of the PEG chains. On the other hand, it is important to highlight that the influence of the repulsion forces among the COO^- groups on the swelling degree of those samples, which are richer in AAc, was more important than the cross-linking density.

Cytotoxicity research

In vitro cytotoxicity assay was performed to evaluate the pharmacological potential of the hydrogels (Fig. 10). This approach is excellent too in the evaluation of biocompatibility and toxicity of new materials prior to in vivo tests. The cytotoxic concentrations for 50 % of VERO cells (CC_{50}) were determined as the concentration necessary to reduce the cell viability by 50 %. The hydrogels had different effects on the cells. Values for CC_{50} were higher than 150 μg mL^{-1}, indicating that the hydrogels do not have any toxic, destructive constituents for living cells [54, 55]. It is reasonable to say that the proposed hydrogels have acceptable biocompatibility and an appropriate level of security for use in the biological environments.

Conclusions

We developed a pH-responsive hydrogel in which PEG is the key constituent in the polymer network that undergoes degradation by acid-catalyzed hydrolysis. PEG was chemically modified with GMA, and the reaction product was able to undergo radical cross-linking/polymerization with SA and DMAAm. The breakage of the PEG chains in the acidic solutions crumbled the hydrogel structure. This behavior was attributed to acid-catalyzed hydrolysis. All hydrogels showed a pseudo-Fickian behavior, a transport mechanism that occurs when the diffusion coefficient changes with the time and the swelling equilibrium is never fully reached. This characteristic may be important in drug release systems. The PEG-richer hydrogels are less deformable when subjected to compressive stress. With addition of larger amounts of modified PEG, the material became more cross-linked and thus less soft. Results from cytotoxicity showed that the proposed hydrogels may have a great pharmacological potential for use in biological environments. This study offers important information on the synthesis and water transport mechanism of water-swellable networks, being relevant for the development of polymer carriers, although many technological challenges remain ahead.

Acknowledgments E. T. T. N. and M. K. L. T. are grateful to the Coordenação de Aperfeiçoamento de Pessoal de Nivel Superior (CAPES) for a doctorate fellowship. M. R. G. thanks the Conselho Nacional de Desenvolvimento Científico e Tecnológico (CNPq) for post-doctorate fellowship (proc. no. 167432/2013-3). A. F. R. and M. H. K. acknowledge the financial supports given by CNPq, CAPES, Instituto de Ciência, Tecnologia e Inovação em Materiais Complexos e Funcionais (INOMAT), and Fundação Araucária-Brasil.

References

1. Amidon GL, Lee PI, Topp EM (2000) Transport process in pharmaceutical systems. In: Gehrke SH (ed) Synthesis and properties of hydrogels used for drug delivery. Marcel Dekker, Inc, New York, **Cap 13**
2. Warson H (2000) Modern superabsorbent polymer technology. Polym Int 49:1548–1548. doi:10.1002/1097-0126(200011)49:11<1548::AID-PI482>3.0.CO;2-D
3. Tajima H, Yoshida Y, Abiko S, Yamagiwa K (2010) Size adjustment of spherical temperature-sensitive hydrogel beads by liquid–liquid dispersion using a Kenics static mixer. Chem Eng J 156:479–486. doi:10.1016/j.cej.2009.11.010
4. Li Z, Shen J, Ma H, Lu X, Shi M, Li N, Ye M (2013) Preparation and characterization of pH- and temperature-responsive nanocomposite double network hydrogels. Mater Sci Eng C 33:1951–1957. doi:10.1016/j.msec.2013.01.004
5. Chen J, Liu M, Liu H, Ma L, Gao C, Zhu S, Zhang S (2010) Synthesis and properties of thermo- and pH-sensitive poly(diallyldimethylammonium chloride)/poly(N, N-diethylacrylamide) semi-IPN hydrogel. Chem Eng J 159:247–256. doi:10.1016/j.cej.2010.02.034
6. Liu HQ, Zhen M, Wu RH (2007) Ionic-strength- and pH-responsive poly acrylamide-co-(maleilc acid) hydrogel nanofibers. Macromol Chem Phys 208:874–880. doi:10.1002/macp.200600632
7. Althans D, Schrader P, Enders S (2014) Solubilisation of quercetin: comparison of hyperbranched polymer and hydrogel. J Mol Liq 196:86–93. doi:10.1016/j.molliq.2014.03.028
8. Valade D, Wong LK, Jeon YJ, Jia ZF (2013) Monteiro M. J.: polyacrylamide hydrogel membranes with controlled pore sizes. J Polym Sci Part A: Polym Chem 51:129–138. doi:10.1002/pola.26311
9. Hertz J, Robinson R, Valenzuela DA, Layik EB, Goldberg JL (2013) A tunable synthetic hydrogel system for culture of retinal ganglion cells and amacrine cells. Acta Biomater 9:7622–7629. doi:10.1016/j.actbio.2013.04.048
10. Wu YB, Wei W, Zhou M, Wang YQ, Wu J, Ma GH, Su ZG (2012) Thermal-sensitive hydrogel as adjuvant-free vaccine delivery system for H5N1 intranasal immunization. Biomaterials 33:2351–2360. doi:10.1016/j.biomaterials.2011.11.068
11. Truong V, Blakey I, Whittaker AK (2012) Hydrophilic and amphiphilic polyethylene glycol-based hydrogels with tunable degradability prepared by "Click" chemistry. Biomacromolecules 13:4012–4021. doi:10.1021/bm3012924
12. Kono H (2014) Characterization and properties of carboxymethyl cellulose hydrogels crosslinked by polyethylene glycol. Carbohydr Polym 106:84–93. doi:10.1016/j.carbpol.2014.02.020
13. Gavira JA, Cera-Manjarres A, Ortiz K, Mendez J, Jimenez-Torres JA, Patino-Lopez LD, Torres-Lugo M (2014) Use of cross-linked poly(ethylene glycol)-based hydrogels for protein crystallization. Crystal Growth Design 14:3239–3248. doi:10.1021/cg401668z
14. Nguyen MK, Alsberg E (2014) Bioactive factor delivery strategies from engineered polymer hydrogels for therapeutic medicine. Prog

Polym Sci 39:1235–1265. doi:10.1016/j.progpolymsci.2013.12.001

15. Nguyen MK, Jeon O, Krebs MD, Schapira D, Alsberg E (2014) Sustained localized presentation of RNA interfering molecules from in situ forming hydrogels to guide stem cell osteogenic differentiation. Biomaterials 35:6278–6286. doi:10.1016/j.biomaterials.2014.04.048
16. Chen Z, Zhao M, Liu K, Wan YQ, Li XD, Feng G (2014) Novel chitosan hydrogel formed by ethylene glycol chitosan, 1,6-diisocyanatohexan and polyethylene glycol-400 for tissue engineering scaffold: in vitro and in vivo evaluation. J Mater Sci Mater Med 25:1903–1913. doi:10.1007/s10856-014-5223-3
17. Zhu J (2010) Bioactive modification of poly(ethylene glycol) hydrogels for tissue engineering. Biomaterials 31:4639–4656. doi:10.1016/j.biomaterials.2010.02.044
18. Domb AJ, Amselem S, Langer R, Maniar M (1994) Polyanhydrides as carriers of drugs in biomedical polymers: designed-to-degrade systems, Shalaby, S. W., Ed., Hanser Publishers, chap. 3
19. Shalaby W, KJL Burg (2004) Absorbable and biodegradable polymers: cyanoacrylate-based systems as tissue adhesives, Shalaby W. Shalaby and Waleed S. W. Shalaby, Ed. CRC Press, chap. 5
20. Sitta DLA, Guilherme MR, da Silva EP, Valente AJM, Muniz EC, Rubira AF (2014) Drug release mechanisms of chemically cross-linked albumin microparticles: effect of the matrix erosion. Colloids Surf B: Biointerfaces 122:404–413. doi:10.1016/j.colsurfb.2014.07.014
21. Burek M, Czuba ZP, Waskiewicz S (2014) Novel acid-degradable and thermo-sensitive poly(N-isopropylacrylamide) hydrogels cross-linked by α, α-trehalose diacetals. Polymer 55:6460–6470. doi:10.1016/j.polymer.2014.10.032
22. Scott JE (1995) Extracellular matrix, supramolecular organisation and shape. J Anat 187:259–269
23. Kunita MH, Guilherme MR, Filho LC, Muniz EC, Franceschi E, Dariva C, Rubira AF (2011) Solid-state radical grafting reaction of glycidyl methacrylate and poly(4-methyl-1-pentene) in supercritical carbon dioxide: surface morphology and adhesion. J Colloid Interface Sci 361:331–337. doi:10.1016/j.jcis.2011.05.024
24. Contreras-Lopez D, Saldivar-Guerra E, Luna-Barcenas G (2013) Copolymerization of isoprene with polar vinyl monomers: reactivity ratios, characterization and thermal properties. Eur Polym J 49:1760–1772. doi:10.1016/j.eurpolymj.2013.03.030
25. Wang SS, Shao L, Song ZQ, Zhao JR, Feng Y (2012) Preparation of epoxy functionalized PP with unique structure and its post-ring open reaction. J Appl Polym Sci 124:4827–4837. doi:10.1002/app.35569
26. Reis AV, Fajardo AR, Schuquel ITA, Guilherme MR, Vidotti GJ, Rubira AF, Muniz EC (2009) Reaction of glycidyl methacrylate at the hydroxyl and carboxylic groups of poly(vinyl alcohol) and poly(acrylic acid): is this reaction mechanism still unclear? J Organic Chem 74:3750–3757. doi:10.1021/jo900033c
27. Wang XR, Shen YD, Lai XJ (2014) Micromorphology and mechanism of polyurethane/polyacrylate membranes modified with epoxide group. Progress Organic Coatings 77:268–276. doi:10.1016/j.porgcoat.2013.09.013
28. Liu X, Xiang S, Yue YM, Su X, Zhang W, Song C, Wang P (2007) Preparation of poly(acrylamide-co-acrylic acid) aqueous latex dispersions using anionic polyelectrolyte as stabilizer. Colloids Surf A Physicochem Eng Asp 311:131–139. doi:10.1016/j.colsurfa.2007.06.007
29. Soucek MD, Yi Y (2011) Synthesis and characterization of water soluble carboxymethyl chitosan grafted with glycidyl methacrylate. J Macromol Sci, Part A: Pure Appl Chem 48:562–568. doi:10.1080/10601325.2011.579819
30. Kolya H, Tripathy T (2013) Grafted polysaccharides based on acrylamide and N, N-dimethylacrylamide: preparation and investigation of their flocculation performances. J Appl Polym Sci 127:2786–2795. doi:10.1002/app.37603
31. Kolya H, Tripathy T (2013) Hydroxyethyl starch-g-poly-(N, N-dimethylacrylamideco-acrylic acid): an efficient dye removing agent. Eur Polym J 49:4265–4275. doi:10.1016/j.eurpolymj.2013.10.012
32. Crockford C, Geen H, Titman JJ (2001) Two-dimensional MAS-NMR spectra which correlate fast and slow magic angle spinning sideband patterns. Chem Phys Lett 344:367–373. doi:10.1016/S0009-2614(01)00820-X
33. Hung I, Gan ZH (2011) An efficient amplification pulse sequence for measuring chemical shift anisotropy under fast magic-angle spinning. J Magn Reson 213:196–199. doi:10.1016/j.jmr.2011.09.015
34. Shahid SA, Qidwai AA, Anwar F, Ullah I, Rashid U (2012) Improvement in the water retention characteristics of sandy loam soil using a newly synthesized poly(acrylamide-co-acrylic Acid)/$AlZnFe_2O_4$ superabsorbent hydrogel nanocomposite material. Molecules 17:9397–9412. doi:10.3390/molecules17089397
35. Rashidzadeh A, Olad A, Salari D, Reyhanitabar A (2014) On the preparation and swelling properties of hydrogel nanocomposite based on sodium alginate-g-Poly (acrylic acid-co-acrylamide)/Clinoptilolite and its application as slow release fertilizer. J Polym Res 21:1–15. doi:10.1007/s10965-013-0344-9
36. Çaykara T, Akçakaya İ (2006) Synthesis and network structure of ionic poly(N, N-dimethylacrylamide-co-acrylamide) hydrogels: comparison of swelling degree with theory. Eur Polym J 42:1437–1445. doi:10.1016/j.eurpolymj.2006.01.001
37. Patel YN, Patel MP (2013) A new fast swelling poly DAPB-co-DMAAm-co-AASS superabsorbent hydrogel for removal of anionic dyes from water. Chin Chem Lett 24:1005–1007. doi:10.1016/j.cclet.2013.06.009
38. Li PC, Xu K, Tan Y, Lu CG, Li YL, Wang PX (2013) A novel fabrication method of temperature-responsive poly(acrylamide) composite hydrogel with high mechanical strength. Polymer 54:5830–5838. doi:10.1016/j.polymer.2013.08.019
39. Poon YF, Cao Y, Zhu Y, Judeh ZMA, Chan-Park MB (2009) Addition of β-malic acid-containing poly(ethylene glycol) dimethacrylate to form biodegradable and biocompatible hydrogels. Biomacromolecules 10:2043–2052. doi:10.1021/bm801367n
40. Giammona G, Pitarresi G, Craparo EF, Cavallaro G, Buscemi S (2001) New biodegradable hydrogels based on a photo-cross-linkable polyaspartamide and poly(ethylene glycol) derivatives. Release studies of an anticancer drug. Colloid Polym Sci 279:771–783. doi:10.1007/s003960100492
41. Lee CY, Teymour F, Camastral H, Tirelli N, Hubbell JA, Elbert DL, Papavasiliou G (2014) Characterization of the network structure of PEG diacrylate hydrogels formed in the presence of N-vinyl pyrrolidone. Macromol React Eng 8:314–328. doi:10.1002/mren.201300166
42. Siepmann J, Peppas NA (2001) Modeling of drug release from delivery systems based on hydroxypropyl methylcellulose (HPMC). Adv Drug Deliv Rev 48:139–157. doi:10.1016/S0169-409X(01)00112-0
43. Dokoumetzidis A, Papadopoulou V, Macheras P (2006) Analysis of dissolution data using modified versions of Noyes-Whitney equation and the Weibull function. Pharm Res 23:256–261. doi:10.1007/s11095-006-9093-3
44. Costa P, Sousa Lobo JM (2001) Modeling and comparison of dissolution profiles. Eur J Pharm Sci 13:123–133. doi:10.1016/S0928-0987(01)00095-1
45. Papadopoulou V, Kosmidis K, Vlachou M, Macheras P (2006) On the use of the Weibull function for the discernment of drug release mechanisms. Int J Pharm 309:44–50. doi:10.1016/j.ijpharm.2005.10.044

46. Costa D, Valente AJM, Miguel MG, Queiroz J (2011) Gel network photodisruption: a new strategy for the codelivery of plasmid DNA and drugs. Langmuir 27:13780–13789. doi:10.1021/la2026285
47. Altaf K, Ashcroft IA, Saleh N, Hague R (2012) Environmental aging of epoxy based stereolithography parts Part 1-Moisture transport. Plastics Rubber Composites 41:120–128. doi:10.1179/1743289811Y.0000000024
48. Katoch S, Sharma V, Kundu PP (2010) Water sorption and diffusion through saturated polyester and their nanocomposites synthesized from glycolyzed PET waste with varied composition. Chem Eng Sci 65:4378–4387. doi:10.1016/j.ces.2010.03.050
49. Wu QX, Li MZ, Yao SJ (2014) Performances of NaCS-WSC protein drug microcapsules with different degree of substitution of NaCS using sodium polyphosphate as cross-linking agent. Cellulose 21:1897–1908. doi:10.1007/s10570-014-0209-3
50. Song F, Wang XL, Wang YZ (2011) Poly (N-isopropylacrylamide)/poly (ethylene oxide) blend nanofibrous scaffolds: thermoresponsive carrier for controlled drug release. Colloids Surf B: Biointerfaces 88:749–754. doi:10.1016/j.colsurfb.2011.08.015
51. Curcio M, Altimari I, Spizzirri UG, Cirillo G, Vittorio O, Puoci F, Picci N, Iemma F (2013) Biodegradable gelatin-based nanospheres as pH-responsive drug delivery systems. J Nanoparticles Res 15:1581. doi:10.1007/s11051-013-1581-x
52. Xu T, Farris RJ (2006) Stresses associated with diffusion in polyimide and polyacrylics films. J Appl Polym Sci 99:2661–2670. doi:10.1002/app.22807
53. Wind MM, Lenderink HJW (1996) A capacitance study of pseudo-Fickian diffusion in glassy polymer coatings. Progress Organic Coatings 28:239–250. doi:10.1016/0300-9440(95)00601-X
54. Sitta DLA, Guilherme MR, Garcia FP, Cellet TSP, Nakamura CV, Muniz EC, Rubira AF (2013) Covalent albumin microparticles as an adjuvant for production of mucosal vaccines against hepatitis B. Biomacromolecules 14:3231–3237. doi:10.1021/bm400859z
55. da Silva EP, Sitta DLA, Fragal VH, Cellet TSP, Mauricio MR, Garcia FP, Nakamura CV, Guilherme MR, Rubira AF, Kunita MH (2014) Covalent TiO_2/pectin microspheres with Fe_3O_4 nanoparticles for magnetic field-modulated drug delivery. Int J Biol Macromol 67:43–52. doi:10.1016/j.ijbiomac.2014.02.035